Experimental Investigation of Heat Transfer in Separated Flow on a Highly Loaded LP Turbine Cascade

Stefan Wolff, Lars Homeier, Leonhard Fottner
Institut für Strahlantriebe
Universität der Bundeswehr München
D-85577 Neubiberg, Germany
Stefan.Wolff@unibw-muenchen.de

ABSTRACT

Today aerodynamic design tools and CFD-codes provide excellent quality in predicting 2D and 3D flows in turbine components. Nevertheless, correlation and numerical methods are not able to predict heat flux in a satisfactory accuracy for complex heat transfer problems, for example 3D film cooling mixing zones or areas of separated flow.

In order to close part of these gaps in knowledge and to improve the understanding of the interaction between the flow pattern and the heat transfer phenomena, experimental investigations were carried out focused on 2D separated flow on the pressure side leading edge of the highly loaded low pressure turbine cascade named T106-300.

The cascade was instrumented with pressure taps and glue-on hot-film sensors. The pressure taps provided the static profile pressure distribution. The hot-film anemometry technique normally is used to detect boundary layer development; moreover a procedure will be presented to evaluate the heat transfer coefficient as well. Supplementary boundary layer traverses with a 1D hot-wire probe were carried out at positions inside and downstream of the separation.

The dimension of the separation up to 60% chord was varied by the incidence angle. By variation of Reynolds number and Mach number a data set is available which will be put down to a correlation.

NOMENCLATURE

a	[-]	overheat ratio
A	[m^2]	cross-sectional area
b	[m]	gauge width, measurement quantity
d	[-]	incremental displacement
D	[m]	hole diameter
E	[V]	voltage
h	[$W/(m^2K)$]	heat transfer coefficient
I	[A]	electrical current
l	[m]	chord length
m, n	[K/Ω], [K]	coefficients of linear equation $T=f(R)$
P	[W], [-]	power CTA output, probe
$\dot{Q}$	[W]	heat flux
R	[W]	resistance
T	[K]	temperature
Tu	[%]	turbulence level
U	[m/s]	velocity
x	[m]	bi-tangential stream wise co-ordinate
β	[°]	flow angle in circumferential direction
μ_3	[-]	skewness, third order moment

Subscripts

∞	free stream property
0	zero-flow conditions
1, 2	inlet / exit
1..n	indexing number
2th	exit presuming isentropic expansion
c	conductive, property of unheated gauge
cs	cable and support
e	electric
fc	forced convective
L 1;2	leads
P	probe
r	radiation
s	storage
t	total / stagnation
w	property of heated gauge

Abbreviations

BR	Bridge Ratio
CTA	Constant Temperature Anemometry
D	Dimension
HFA	Glue-On Hot-Film Anemometry
HGK	High-Speed Cascade Wind Tunnel
HTC	Heat Transfer Coefficient
HWA	Hot-Wire Anemometry
PPD	Profile Pressure Distribution
PS SS	Pressure Side Suction Side
RMS	Root Mean Square
RP	Reattachment Point
SFC	Specific Fuel Consumption
SP	Separation Point

Paper presented at the RTO AVT Symposium on "Advanced Flow Management: Part B – Heat Transfer and Cooling in Propulsion and Power Systems", held in Loen, Norway, 7-11 May 2001, and published in RTO-MP-069(I).

Report Documentation Page

Form Approved
OMB No. 0704-0188

1. REPORT DATE	2. REPORT TYPE	3. DATES COVERED
00 MAR 2003	**N/A**	**-**

4. TITLE AND SUBTITLE	5a. CONTRACT NUMBER
Experimental Investigation of Heat Transfer in Separated Flow on a Highly Loaded LP Turbine Cascade	5b. GRANT NUMBER
	5c. PROGRAM ELEMENT NUMBER
6. AUTHOR(S)	5d. PROJECT NUMBER
	5e. TASK NUMBER
	5f. WORK UNIT NUMBER
7. PERFORMING ORGANIZATION NAME(S) AND ADDRESS(ES) **NATO Research and Technology Organisation BP 25, 7 Rue Ancelle, F-92201 Neuilly-Sue-Seine Cedex, France**	8. PERFORMING ORGANIZATION REPORT NUMBER
9. SPONSORING/MONITORING AGENCY NAME(S) AND ADDRESS(ES)	10. SPONSOR/MONITOR'S ACRONYM(S)
	11. SPONSOR/MONITOR'S REPORT NUMBER(S)

12. DISTRIBUTION/AVAILABILITY STATEMENT
Approved for public release, distribution unlimited

13. SUPPLEMENTARY NOTES
Also see ADM001490, presented at RTO Applied Vehicle Technology Panel (AVT) Symposium held in Leon, Norway on 7-11 May 2001, The original document contains color images.

14. ABSTRACT

15. SUBJECT TERMS

16. SECURITY CLASSIFICATION OF:			17. LIMITATION OF ABSTRACT	18. NUMBER OF PAGES	19a. NAME OF RESPONSIBLE PERSON
a. REPORT	b. ABSTRACT	c. THIS PAGE			
unclassified	**unclassified**	**unclassified**	**UU**	**10**	

Standard Form 298 (Rev. 8-98)
Prescribed by ANSI Std Z39-18

INTRODUCTION

Due to the demands for more efficient gas turbine, turbine peak cycle temperature increased rapidly in the past enabled by an extensive use of cooling technology. Therefore a lot of research work was conducted within this area, since improvement in material development did not keep up with the thermal requirements. Nevertheless, an increasing turbine inlet temperature comes along with an increasing cooling flow rate. Because of inappropriate accuracy in predicting heat transfer in complex or separated flow the safety margin in cooling design represents a potential to improve SFC.

The present work is part of the European project Aerothermal Investigation on Turbine Endwalls and Blades (AITEB) which focused on the increased ability of cooling technology. The aim is to enable critical parts to withstand higher gas temperatures based on the current cooling flow rate as well as a more accurately predicted component lifetime. This will lead to an improvement in SFC. The objective of the present work is the experimental investigation of a huge 2D separation at the pressure side leading edge of a low pressure turbine blade.

Several works dealt with the problem of flow separation, reattachment and the heat transfer under separated flow on a flat plate like Rivir [10] in addition a collection of paper published by AGARD [1]. Furthermore, a survey of literature provides some studies on more realistic geometries like Pucher and Göhl [8] and Bellows and Mayle [3].

The present investigation was initiated to examine the separated, reattached flow and the interrelated heat transfer at the pressure side leading edge at Mach and Reynolds numbers more appropriate to present low pressure turbines and with a separation covering more then 50% chord. For this investigation an attempt was made to evaluate the HTC from measurements with heated thin-film elements. The use of glue-on hot-film sensors to investigate the heat flux implicates a number of problems, which will be discussed in detail.

EXPERIMENTAL APPARATUS

Turbine cascade

The experimental investigations were performed on a large-scale plane cascade turbine model named T106-300. The cascade consists of three blades with 300 mm chord length and two adjustable tailboards at half pitch distance from the upper and lower blade thus assuring flow periodicity and high spatial resolution together with a two dimensional flow field at mid span. Measurements were carried out exclusively on the centre blade. A sectional sketch and the main aerodynamic and geometric design data are given in Fig. 1.

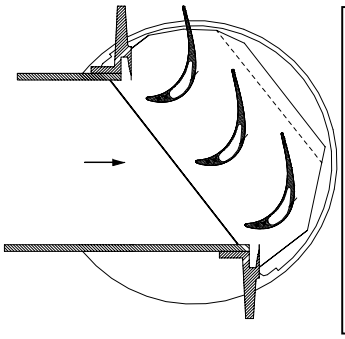

Chord Length:	300 mm
Blade Height:	300 mm
Pitch Ratio:	0.799
Stagger Angle:	59.28°
Ma_1	0.28
Ma_{2th}	0.59
Re_{2th}	500000
β_1	127.70°
β_2	26.70°

Fig. 1 HGK test section with T106-300 cascade

High-Speed Cascade Wind Tunnel

The experiments were carried out at the High-Speed Cascade Wind Tunnel of the Universität der Bundeswehr München (Fig. 2). This wind tunnel is an open loop facility which can operate continuously and reach Mach numbers up to Ma = 1.05 in the test section. Being built inside a large pressurised tank the wind tunnel offers the possibility to vary independently the Mach and the Reynolds number in order to simulate flow conditions, which are typical in modern gas turbines. The total temperature in the settling chamber is set to 303 K. A turbulence generator upstream of the nozzle can adjust the turbulence intensity. The test section exit plane inclination and height can be adjust in order to vary the inlet flow angle. A detailed description of the facility is given in Sturm and Fottner [12].

Instrumentation of the test section

Total temperature (T_{t1}), total pressure (p_{t1}) and static pressure (p_1) in front of the cascade are used for the determination of the inlet flow conditions. The total temperature data is gained in the settling chamber of the wind tunnel (Fig. 2). The static and total pressure is measured 96 mm upstream of the cascade inlet plane. The tank pressure (p_K) is used as reference for all other pressure measurements and characterizes the exit flow conditions.

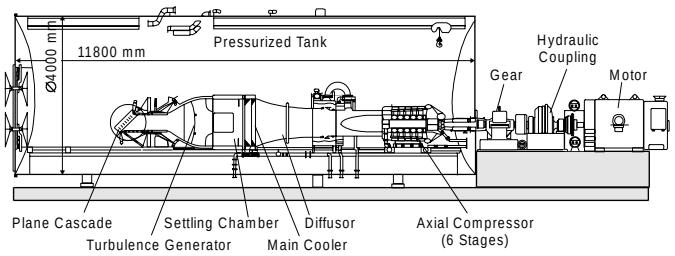

Main test section data:	
Mach Number:	$0.2 \le Ma \le 1.05$
Reynolds Number:	$0.2 \cdot 10^6\ m^{-1} \le Re/L \le 16.0 \cdot 10^6\ m^{-1}$
Inlet Turbulence Level:	$0.4\% \le Tu_1 \le 7.5\%$
Inlet Flow Angle:	$25° \le \beta_1 \le 155°$
Test Section Width:	300 mm
Test Section Height:	235 mm ... 500 mm

Fig. 2 High-Speed Cascade Wind Tunnel

Instrumentation of the test blade

The loading of the cascade is determined by means of static pressure taps in the mid span section of the blade. Altogether 71 pressure taps (PS 24; SS 47) were installed at mid-span. Due to the fact that the centre blade could be exchanged, a second blade was instrumented with an array of 68 *MTU* hot-film gauges which where embedded (glue-on) into the pressure side surface. The array covered the entire pressure side at mid-span.

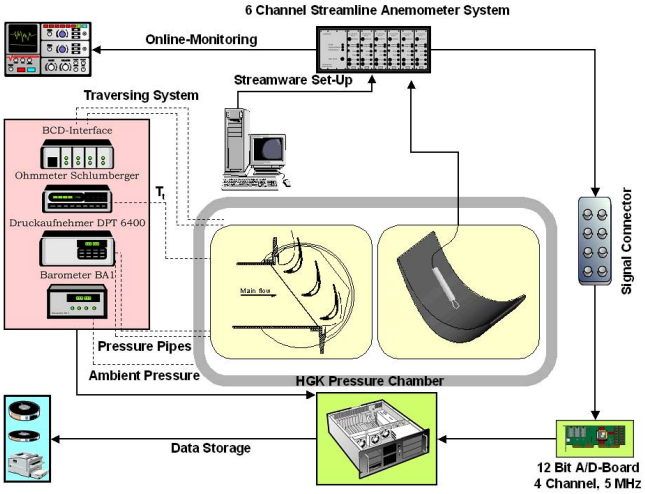

Fig. 3 HWA data acquisition system

Hot-Wire Anemometry (HWA)

The PC based HWA data acquisition system (Fig. 3) is controlled by the in-house developed software *WINSMASH* (Wolff [13]). The boundary layer measurements were conducted using a 1D-HWA probe (*DANTEC HW-55P15*). For each position the probes were calibrated for the local static pressure. The turbulence level in the test section was determined 500 mm upstream of the cascade inlet plane using a hot-film probe (*DANTEC HF-55R01*). A 4th order polynomial has been used for the approximation of the calibration curve.

The HWA signals were low-pass filtered with a cut of frequency of 10kHz. The mean value for a quantity b is given by:

$$\bar{b} = \frac{1}{N}\sum_{j=0}^{N} b_j \qquad (1)$$

where N is the number of samples and b represents the velocity for each sample. The standard deviation of the velocity is calculated using the RMS deviation given by:

$$RMS = \sqrt{\frac{1}{N-1}\sum_{j=0}^{N}(\bar{b} - b_j)^2} \qquad (2)$$

The turbulence level is normalized by the velocity cascade inlet plane U_1:

$$Tu = \frac{RMS}{U_1} * 100\% \qquad (3)$$

Glue-On Hot-Film Anemometry (HFA)

The HFA technique is well established to investigate boundary layer development (e.g. Bellhouse and Schultz [2]). Furthermore, this work is an attempt to evaluate the HTC from the hot-film data. Therefore the hot-film data acquisition system of the Institut für Strahlantriebe (Fig. 4) (Brunner et al. [4]) was adapted and employed.

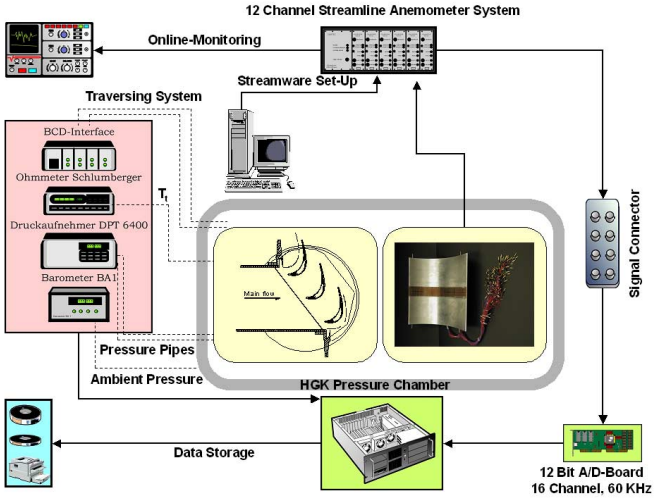

Fig. 4 Layout of the data acquisition system

Two racks of the *DANTEC Streamline* anemometer system, each consisting of 6 anemometers, have been employed. Therefore simultaneous data acquisition of 12 hot-film gauges has been possible. A 12-bit A/D board acquires up to 16 channels simultaneously. The set-up data for each gauge is stored in a project file and is available for further evaluation.

The HFA data are also evaluated with equation 1 and 2 where b represents the anemometer output voltage E. As an additional value the skewness is given as the third order moment:

$$\mu_3(t) = \frac{1}{\bar{b}^3} \cdot \frac{1}{N-1} \cdot \sum_{j=1}^{N}\left(b_j - \bar{b}\right)^3 \qquad (4)$$

Evaluation of Heat Transfer Coefficient

The HFA as well as the HWA is based on the convective heat transfer from the heated sensing element placed in a fluid flow.

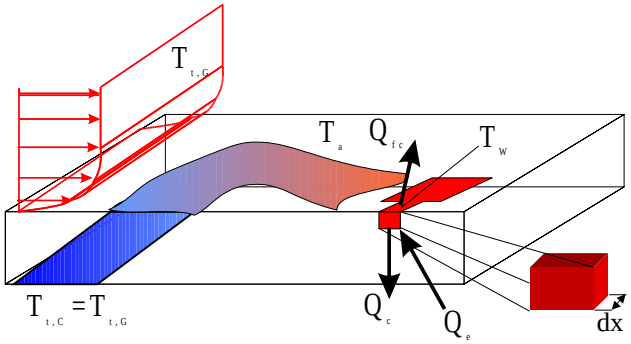

Fig. 5 Heat-rate balance of a glue-on hot-film sensor

The forced convective heat flux $\dot{Q}_{fc}$ can be determined from the heat-rate balance (Fig. 5) equation (cf. Bruun [5]) for an incremental heated film element:

$$d\dot{Q}_e = d\dot{Q}_{fc} + d\dot{Q}_c + d\dot{Q}_s + d\dot{Q}_r \qquad (5)$$

In order to eliminate the terms of radiation, conductive and storage heat flux, a measurement is conducted under zero flow conditions at the same overheat ratio:

$$d\dot{Q}_{e;0} = d\dot{Q}_{fc;0} + d\dot{Q}_{c;0} + d\dot{Q}_{r;0} + d\dot{Q}_{s;0} \qquad (6)$$

Consider that:

$$d\dot{Q}_{fc;0} = 0$$
$$d\dot{Q}_{c;0} = d\dot{Q}_c \;;\; d\dot{Q}_{r;0} = d\dot{Q}_r \;;\; d\dot{Q}_{s;0} = d\dot{Q}_s \qquad (7)$$

The forced convective heat flux is determined as:

$$d\dot{Q}_{fc} = d\dot{Q}_e - d\dot{Q}_{e;0} \qquad (8)$$

The forced convective heat flux can be expressed as well in terms of the HTC h:

$$d\dot{Q}_{fc} = dh\, b\,(T_w - T_c)dx \qquad (9)$$

Assuming that h is constant in x-direction, $\dot{Q}_{fc}$ results in:

$$\dot{Q}_{fc} = h\,A\,(T_w - T_c) \qquad (10)$$

The heat generation rate by an electrical current I of the hot-film with a resistance R_w given by:

$$\dot{Q}_e = I\,R_w = \frac{E_w^2}{R_w} \qquad (11)$$

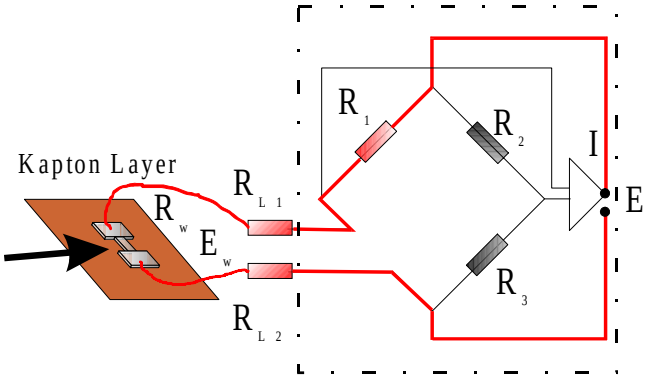

Fig. 6 Schematic of CTA Wheatstone bridge with hot-film

The voltage drop over the gauge can be determined by the Kirchhoff´s laws for the electric cycle of the gauge arm shown in Fig. 6:

$$E_w = \frac{R_w}{R_1 + R_{L1} + R_w + R_{L2}} E \qquad (12)$$

where E is the bridge output voltage.

The fixed resistance R_1 and the bridge ratio $BR=R_2/R_1$ is given by the vendor of the anemometer system. To determine the leads resistance of the connecting flags and wires from the gauges to the CTA input R_{L1} and R_{L2}, one of the gauges is connected with two leads on both connecting flags. This electric cycle can be used as a shorting probe.

However, it is not possible to measure the resistance of the heated gauge R_w under operating conditions, but the resistance can be determined considering the bridge set-up procedure:

1. Measuring the cold resistance of the probe R_P at T_c
2. Calculating the cold resistance of the gauge by subtracting the resistance of the connecting wires

$$R_c = R_P - R_{L1} - R_{L2} \qquad (13)$$

3. Calculating the hot resistance of the gauge by setting the overheat ratio a:

$$R_w = (1+a)\,R_c \qquad (14)$$

4. Calculating the overheat resistance of the probe

$$R_{P,w} = R_w + R_{L1} + R_{L2} \qquad (15)$$

5. Setting the decade resistance R_3 of the adjust arm of the bridge by the bridge ratio BR:

$$R_3 = BR\,R_{P,w} \qquad (16)$$

For CTA mode R_w is kept constant when the bridge is in balance. The same set-up procedure is done for the zero flow measurement.

Using equation 4, 6 and 7 the HTC h can be calculated as:

$$h = \left(\frac{E_w^2}{R_{w,h}} - \frac{E_{w,0}^2}{R_{w,0,h}} \right) \frac{1}{A(T_w - T_\infty)} \qquad (17)$$

The driving temperature difference is defined as the difference between the heated gauge under flow conditions T_w and the free stream temperature T_∞. The free stream temperature is calculated using the profile pressure distribution and the total temperature determined in the settling chamber.

The temperature of the heated gauge can be determined by calibrating the temperature sensitivity of the gauge resistance. Therefore the instrumented blade was subjected to five different temperatures and the resistance of each gauge was measured and tabled. The resistant was found to be linear in the range of temperatures. Related to this calibration measurement the temperature of the gauge can be calculated as:

$$T_W = m R_W + n = m (1 + a) R_C + n \qquad (18)$$

Where m, n are the linear coefficients determined by the calibration measurement.

It should be noted, that there are several aspects, that have to be considered using heated thin-films to determine the HTC. First of all, the heated element represents a local step in the wall temperature, which implicates as well a step on the HTC (cf. Heselhaus [7]). Work is going on in order to find a solution by superposing this problem with a standard flat plate with a wall temperature step in order to correct the HTC to get an adequate engineering accuracy (cf. Reynolds et al [9]). Some of the assumption that was made to evaluate the HTC has to be reconsidered. The main problem arises with the assumption in equation (7) that the heat conduction into the blade material is constant. Haselbach [6] dealt with heat balance and the calibration of heated thin-films for skin friction measurements. He pointed out that a part of the conductive heat loss convects indirectly into the flow via the substrate. He stated that this process is coupled with the flow conditions, which also affects the effective wetted area of heat exchange. Work is going on for this problem in order to examine carefully the effects on the present results respectively to find a way to eliminate this interaction.

EXPERIMENTAL RESULTS

The experiments were conducted for different inflow conditions listed in Tab. 1. The numbers inside the brackets are the number of boundary layer traverses.

	$\beta_1 = 127.7°$	$\beta_1 = 105.0°$	$\beta_1 = 90.0°$
$Re_{2th} = 150000$ $Ma_{2th} = 0.5$	PPD, HFA, HWA (5)	PPD, HFA, HWA (7)	PPD, HFA, HWA (6)
$Re_{2th} = 200000$ $Ma_{2th} = 0.5$			PPD, HFA, HWA (6)
$Re_{2th} = 500000$ $Ma_{2th} = 0.59$	PPD, HFA		

Tab. 1. Test program

The turbulence level in the test section upstream of the cascade inlet plane was determined to be $Tu_1 = 3.4\%$ for $Re_{2th} = 150000$ and $Tu_1 = 3.6\%$ for $Re_{2th} = 200000$.

For the discussion of the results a definition of the separation and reattachment point is necessary. The separation and the reattachment point are defined as a point of singularity, where the sign of velocity near to the wall changes.

Numerical results

In order to get an impression of the flow pattern, numerical results for different inflow angles are shown in Fig. 7. For the design angle the stream traces follow the pressure side contour. For an incidence of 22.7° the flow on the pressure side separates directly at the leading edge and reattaches at about 30% chord. For an incidence angle of 37.7° a huge separation can be seen and the flow reattaches at about 60% chord.

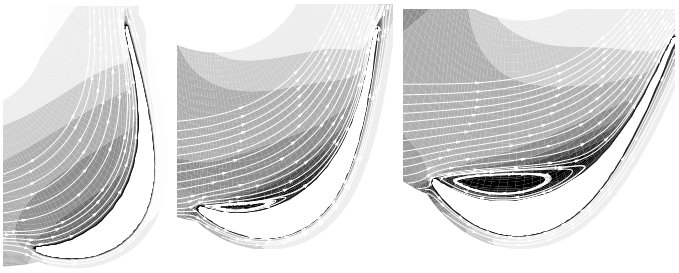

β_1=127.7° β_1=105.0° β_1=90.0°

Fig. 7 CFD flow pattern ($Ma_{2th} = 0.5$, $Re_{2th} = 150000$)
NUMECA Ingenieurbüro Dr.-Ing. Hildebrandt

Blade Loading

In Fig. 8 the profile pressure coefficient is given for all investigated inflow conditions. For the design point ($Re_{2th} = 500000$, $Ma_{2th} = 0.59$, $\beta_1 = 127.7°$, circles) the pressure coefficient shows a strong acceleration on the suction side up to 40% chord. A laminar separation bubble is detected at 70 % chord. On the pressure side a suction peak with a gentle deceleration at the leading edge can be observed. Further downstream the acceleration increases up to the trailing edge. For the case of lower Re- and Ma-number (squares) the PS looks like the same but the acceleration and the separation on the SS is stronger.

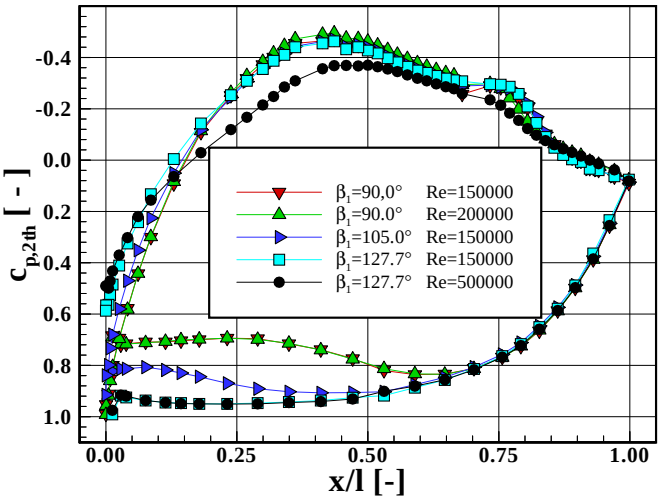

Fig. 8 **Profile pressure coefficient**

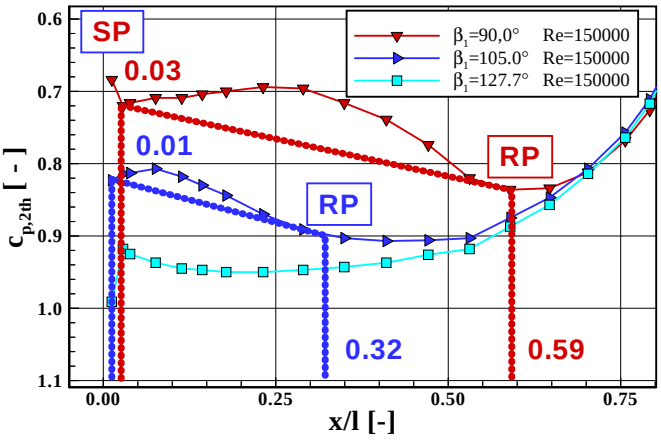

Fig. 9 **Detection of the reattachment point**

In order to detect the Separation Point (SP) and the Reattachment Point (RP) a zoom on the PS pressure coefficient is shown in Fig. 9. The SP is defined as the beginning of the area of zero pressure gradient. The RP is defined as the intersection of the tangent originated at the SP to the graph. For $\beta_1 = 90°$ the SP is located at x/l = 0.03 and the RP at x/l = 0.59. For $\beta_1 = 105°$ the flow separates nearly at the same position whereas the separation is far smaller with the RP at x/l = 0.32. For the variation of the Re-number for $\beta_1 = 90°$ no influence was detected.

Taking into account that it is problematically to determine the RP only with the pressure coefficient distribution, a look at other measurement results will help to validate the statements.

HWA Results

In order to get useful results the axial positions of the HWA measurements were defined after detecting the dimension of the separation. Therefore velocity and turbulence profiles inside the separation, in the vicinity of the reattachment as well as for the reattached boundary layer are provided. The velocity and turbulence vectors (the traverses are perpendicular to the surface) represent the absolute value turned into surface tangential direction.

In Fig. 11 and Fig. 12 the velocity profiles are given for $\beta_1 = 105.0°$ and $\beta_1 = 90.0°$ at $Ma_{2th} = 0.5$, $Re_{2th} = 150000$. It should be noted that a single hot-wire cannot by itself sense the direction of the flow, therefore the velocity data in the separation were plotted as measured. One might expect that the absolute value of the velocity converge zero in the centre of the separation. But behaviour like this was not detected and there are two possible reasons for that. First of all the accuracy of the calibration for such low velocities at a static pressure level of about 5000 Pa is not reasonable. On the other hand, a separation is an unsteady phenomena and it should be impossible to detect the streamline of zero velocity inside the separation. For $\beta_1 = 105.0°$ the velocity profiles up to x/l = 0.25 shows a region of 'reverse' flow. The boundary layer reattaches between x/l = 0.25 and x/l = 0.35 and the profile at x/l = 0.35 is characteristic for reattached boundary layers. The profiles further downstream show the characteristics of an attached accelerated boundary layer.

The profiles for $\beta_1 = 90.0°$ (Fig. 12) indicate a far bigger separation. The profile at x/l = 0.18 shows a local minimum which denotes the middle of the separation with the change in velocity direction. Closer to the wall the reverse flow velocity accelerates to a local maximum and decelerates again closer to the wall. The same profile patterns can be detected for x/l = 0.35 but the local minimum shifted closer to the wall. Somewhere between x/l = 0.55 and x/l = 0.60 the flow reattaches and further downstream at x/l = 0.68 an attached profile was detected.

The corresponding turbulence profiles are displayed in Fig. 14 and Fig. 15. Within the undisturbed channel flow the turbulence level was determined between 4% and 5%. It is visible that the maximum level of turbulence was detected at the border of the separation. Especially for $\beta_1 = 105°$ at x/l = 0.05 (Fig. 14) the peak in this region stands out clearly. Further downstream the gradient in surface normal direction decreases. But the turbulence seems to be transported through the channel. The turbulence production of the shear layers due to the separation are dominating so that a normal distribution with a maximum directly at the wall cannot be found until x/l = 0.55. For $\beta_1 = 90°$ the distributions are similar.

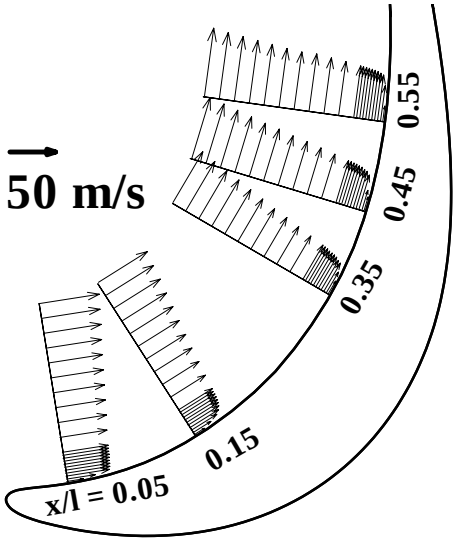

Fig. 10 HWA velocity profiles: $\beta_1 = 127.7°$

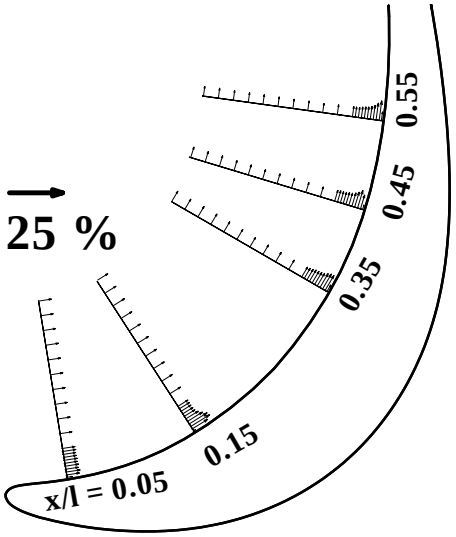

Fig. 13 HWA turbulence profiles: $\beta_1 = 127.7°$

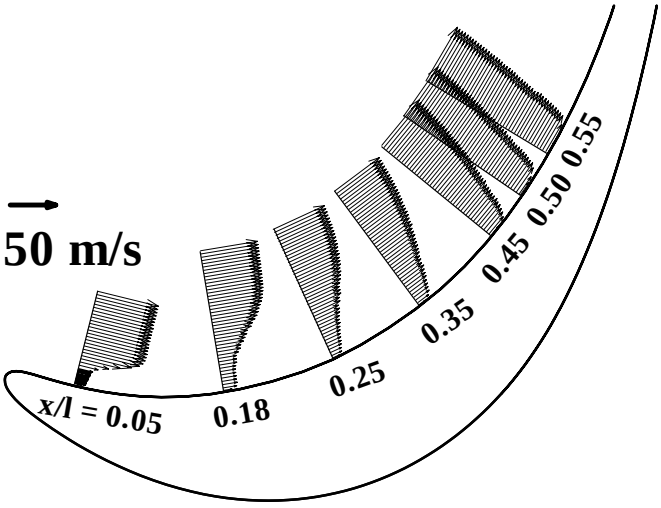

Fig. 11 HWA velocity profiles: $\beta_1 = 105.0°$

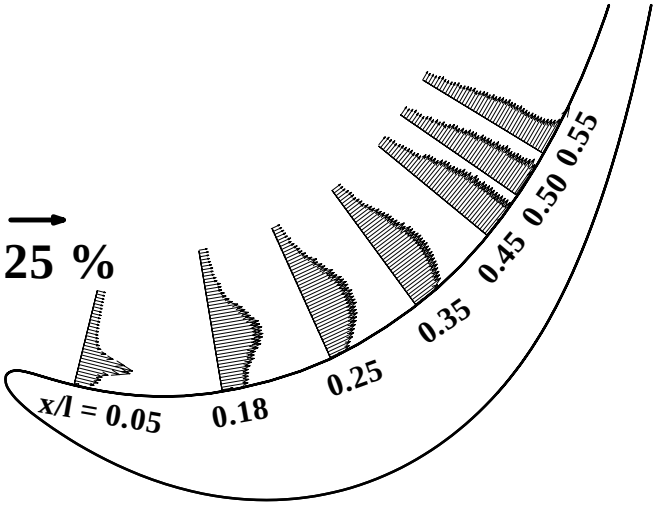

Fig. 14 HWA turbulence profiles: $\beta_1 = 105.0°$

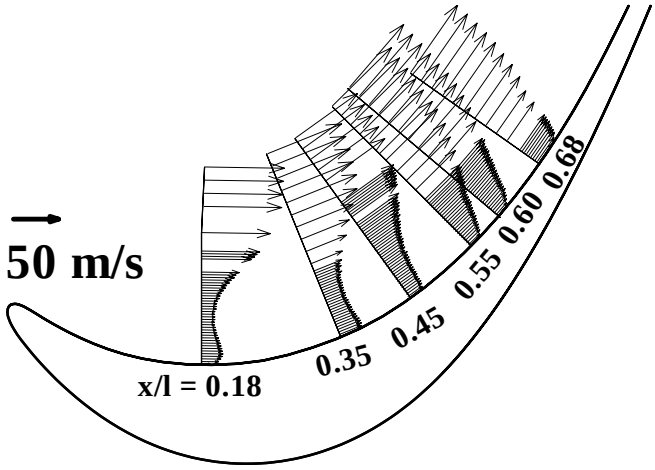

Fig. 12 HWA velocity profiles: $\beta_1 = 90.0°$

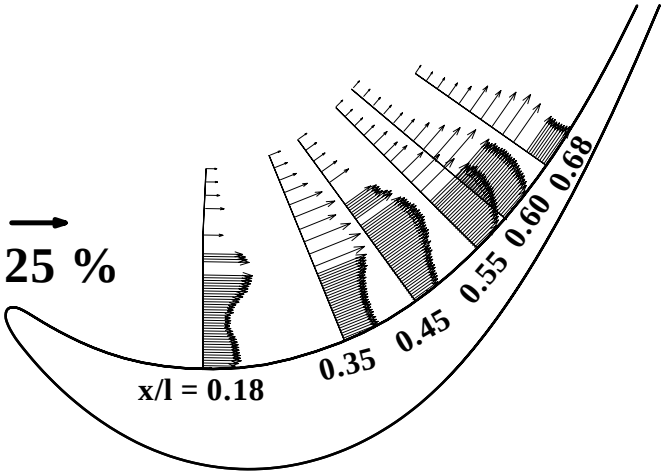

Fig. 15 HWA turbulence profiles: $\beta_1 = 90.0°$

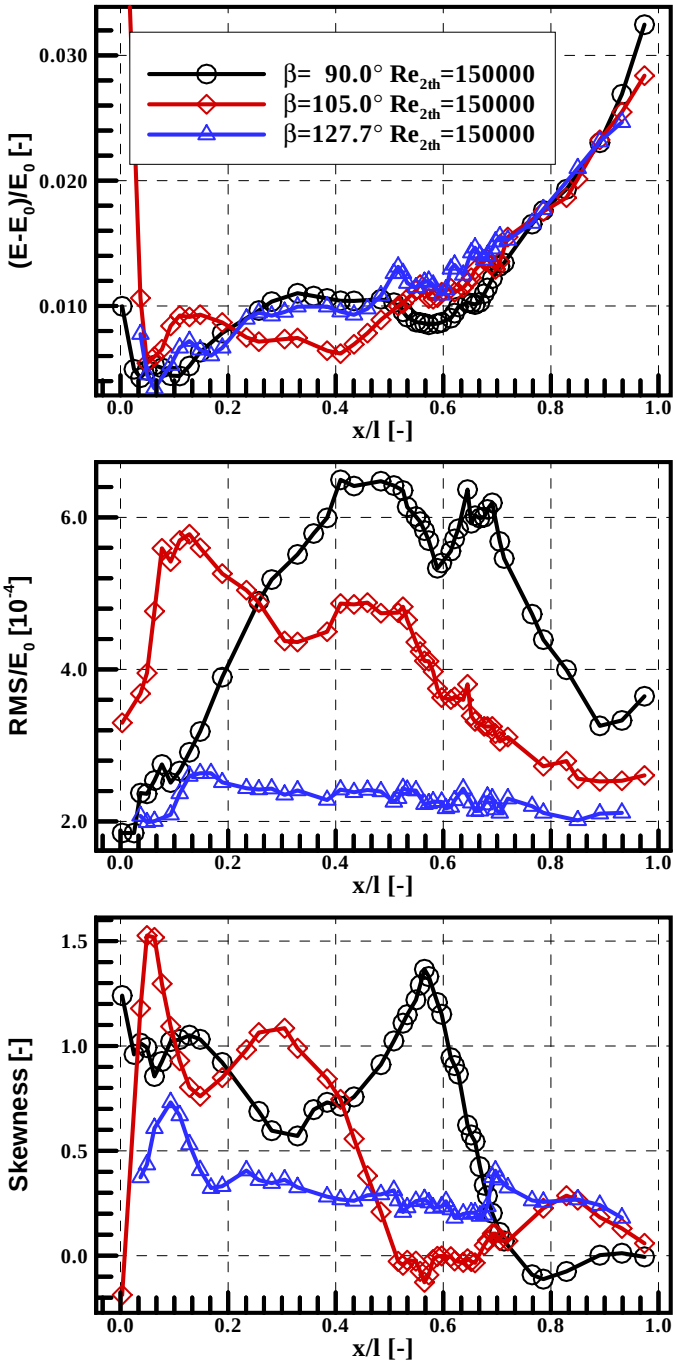

Fig. 16 HFA results of boundary layer conditions for Re_{2th} = 150000, Ma_{2th} = 0.5

HFA results

The HFA results are predestined to detect flow phenomena like separation and transition (e.g. Schröder et al. [11], Bellhouse et al. [2]). However, not all of their guidelines to discuss the results are valid for pressure side separated flow, too. In order to detect the reattachment location the quasi wall shear stresses, the dimensionless RMS value and the skewness for Re_{2th} = 150000 are displayed in Fig. 16.

For $\beta_1 = 90°$ a local minimum for the quasi wall shear stress and the RMS value is detected at x/l = 0.59 and indicates the reattachment point. The same pattern can be observed for $\beta_1 = 105°$ at x/l = 0.32. Downstream of x/l = 0.5 for $\beta_1 = 105°$ and x/l = 0.7 for $\beta_1 = 90°$ the values of wall shear stress are the same as for the design angle. At these positions the profile pressure distributions converges as well.

The RMS values for the separated flow are much higher than for the attached flow. A gentle increase in RMS value for the design angle was detected downstream of the suction peak due to the adverse pressure gradient. Further downstream the value decreases continuously. For the other angles the RMS value increases inside the separation to a maximum close to the reattachment location. A second peak in RMS values can be observed downstream of the reattachment due to the transportation of the shear layer turbulence closer to the wall. When the flow accelerates the RMS level decreases rapidly. It has to be stated that the RMS level for the cases with separated flow close to the trailing edge is higher than for the case of attached flow.

The absolute maximum of the skewness for both off design angles was detected almost at the reattachment point just shifted slightly upstream. The zero crossing of the skewness for both off design angles coincidences with the point where the flow is accelerated again (e.g. Fig. 9) and the quasi wall shear stresses converges the distribution for the design angle.

Preliminary heat transfer results

The results for the local HTC are displayed in Fig. 17. In the first figure the HTC for $\beta_1 = 90°$ is compared to $\beta_1 = 127.7°$. For both angles the HTC reaches the minimum at x/l = 0.05. For $\beta_1 = 127.7°$ a local maximum is detected just downstream of the suction peak and the HTC increases rapidly when the flow is accelerated. The heat transfer for the separated flow comes to a maximum in the middle of the separation and to a local minimum at the reattachment point. However, the HTC for the separated flow is in the same order than for the attached flow and at the reattachment point it is even less. For the smaller separation ($\beta_1 = 105°$) the HTC shows a local maximum in the middle of the separation and a local minimum at the reattachment point, too. Furthermore, a small peak was detected just downstream of the reattachment location due to the high turbulent shear layers transported closer to the wall. Between the reattachment and the point where the profile pressure distributions converge ($0.3 \le x/l \le 0.5$) the HTC for the case with separation is lower than for the design case.

CONCLUSION

A separation which covers 30% respectively 60% chord at the leading edge pressure side of a highly loaded

low pressure turbine cascade was generated by a large incidence. The boundary layer was investigated using standard pressure taps and 1D HWA as well as glue-on hot-film sensors for appropriate Mach and Reynolds numbers. Furthermore, a proposal was presented to evaluate HTC from heated thin-film measurements and specific problems were discussed. The detected HTC increases inside the separation with a, unlike to previous studies, local minimum in the reattachment region. The HTC for the separated and reattached flow was determined not to be higher as for the design angle.

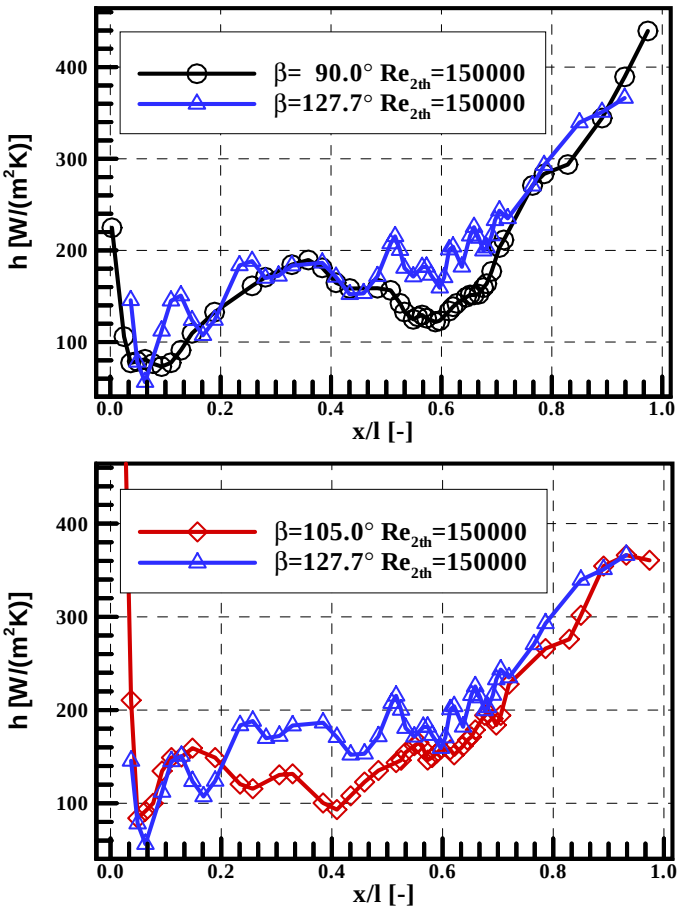

Fig. 17 Local HTC

ACKNOWLEDGMENTS

The reported work was performed within a research project that is part of the European project Aerothermal Investigation on Turbine Endwalls and Blades (AITEB – Contract - Number: G4RD-CT-1999-00055). The permission for publication is gratefully acknowledged. The author gratefully acknowledges as well the CFD support by NUMECA Ingeneurbüro Dr.-Ing. Thomas Hildebrandt as the experimental work by Lt. Dipl.-Ing. Matthias Klein.

REFERENCES

1. AGARD, 1976, “Flow Separation”, AGARD-CP-168
2. Bellhouse, B.J., Schultz, D.L. 1966, “Determination of mean and dynamic skin friction, separation and transition in low-speed flow with a thin-film heated element“, J. of Fluid Mech. 1966 Vol. 24
3. Bellows, W.J., Mayle, R.E, 1986, “Heat Transfer Downstream of a Leading Edge Separation Bubble“, ASME 86-GT-59
4. Brunner, S., Teusch, R., Stadtmüller, P., Fottner, L., 1998, “The Use of Simultaneous Surface Hot Film Anemometry to Investigate Unsteady Wake Induced Transition in Turbine and Compressor Cascades“, 14th Symposium on Measuring Techniques
5. Bruun, H., 1995, “Hot-Wire Anemometry: Principles and Signal Analysis“, Oxford University Press
6. Haselbach, F., 1997, “Thermalhaushalt und Kalibration von Oberflächenheißfilmen und Heißfilmarrays“, Fortschritt-Berichte VDI: Reihe 7 Nr. 326
7. Heselhaus, A., 1997, “Ein hybrides Verfahren zur gekoppelten Berechnung von Heißgasströmung und Materialtemperaturen am Beispiel gekühlter Turbinenschaufeln“, Doctoral Thesis Rur-Universität Bochum
8. Pucher, P., Göhl., R., 1986, “Experimental Investigation of Boundary Layer Separation with Heated Thin-Film Sensors”, ASME 86-GT-254
9. Reynolds, W.C., Kays, W.M., Kline, S.J., 1958, “Heat Transfer in the turbulent incompressible Boundary Layer: III – Arbitrary Wall Temperature and Heat Flux”, NASA Memorandum 12-3-58W
10. Rivir, R.B., Johnston, J.P., Eaton, J.K., 1992, “Heat Transfer on a Flat Surface Under a Region of Turbulent Separation”, ASME 92-GT-198
11. Schröder, T., Haueisen, V., Hennecke, D., 1998, “Measurements with Surface Mounted Hot-Film Sensors on Boundary Layer Transition in Wake Disturbed Flow”, AGARD CP-598, Nr. 38
12. Sturm, W., Fottner , L., 1985, “The High-Speed Cascade Wind Tunnel of the German Armed Forces University Munich“, 8th Symposium on Measuring Techniques in Transonic and Supersonic Flows in Cascades and Turbomachines
13. Wolff, S., 1999, “Konzeption, Programmierung und Erprobung eines PC-gesteuerten Meßsystems zur Aufnahme und Auswertung von 1-D und 3-D-Hitzdraht-Signalen am Hochgeschwindigkeits-Gitterwindkanal als Ersatz des HP-Systems“, Institute Report WOIB9909

Paper Number: 15

Name of Discusser: H. B.Weyer, DLR Cologne

Question:
Is the conclusion correct, that hot wire anemometry (HWA) is not fully appropriate to measure the flow inside the bubble, in particular the reattachment point?
Would you believe the planar laser anemomentry would be advantageous?

Answer:
The conclusion is correct and for sure a non intrusive measurement technique which is able to measure low velocities could be advantageous. However, for LDA or L2F an optical access over the entire 300 mm chord is necessary.
Nevertheless, most of the measurements has been carried out in the reattached region and in this case the HWA is an appropriate tool to get information especially on the turbulence level. Furthermore, the HWA was not mainly used to detect the reattachment point.